Novel Coupling Schemes for Microwave Resonator Filters

Uwe Rosenberg, *Senior Member, IEEE*, and Smain Amari, *Member, IEEE*

***Abstract*—This paper introduces novel coupling schemes for microwave resonator filters. It is shown that higher order filter characteristics can be obtained from lower order sections, which are connected in parallel between the source and load, by proper superposition of the individual lower order responses. This property can be used in modular filter design by focusing on separate sections of the filter one at a time. In addition, some of these coupling schemes exhibit zero-shifting properties, whereby transmission zeros can be shifted from one side of the passband to the other by simply changing the resonant frequencies of the resonators while keeping all the coupling coefficients unchanged. Several novel filter designs of different kinds (microstrip, planar waveguide cavity, and dual-mode types) are introduced to prove the new method and to give an idea of the extended design possibilities. Good agreement between measured, computed, and synthesized results is demonstrated.**

***Index Terms*—Bandpass filters, design, dual-mode filters, elliptic filters, N-path filters, resonator filters, synthesis.**

I. Introduction

THE synthesis and design of elliptic and pseudoelliptic coupled resonator filters is important for channel separation components in modern communication systems. Filtering structures for these systems are required to provide sharp cutoff slopes, asymmetric responses, and equalized group delay. All these features can be successfully achieved by filters with transmission zeros at finite frequencies in the complex plane.

An examination of the synthesis techniques available in the literature shows that elliptic and pseudoelliptic filters are considered as perturbed versions of the all-pole Chebyshev solution for a filter of the same order, center frequency, bandwidth, and ripple level. The perturbation, which takes the form of cross or bypass couplings, is responsible for bringing the transmission zeros from infinity to finite positions in the complex plane. In particular, the coupling and routing scheme of these filters always include a main path in which the ith and $(i+1)$th resonators are directly coupled with relatively strong direct or main couplings [1]–[5]. Fig. 1(b) depicts in principle the conventional coupling scheme for a four-pole elliptic function filter design. The relatively weak cross-coupling between resonators 1 and 4 is introduced to generate a symmetrical pair of finite transmission zeros. The direct couplings are stronger than the cross-coupling term unless the transmission zeros are located very close to the passband.

Manuscript received April 5, 2002; revised August 9, 2002.

U. Rosenberg is with Marconi Communications GmbH, Backnang D-71522, Germany (e-mail: Uwe.Rosenberg@ieee.org).

S. Amari is with the Department of Electrical and Computer Engineering, Royal Military College of Canada, Kingston, ON, Canada K7K 7B4 (e-mail: smain.amari@rmc.ca).

Digital Object Identifier 10.1109/TMTT.2002.805171

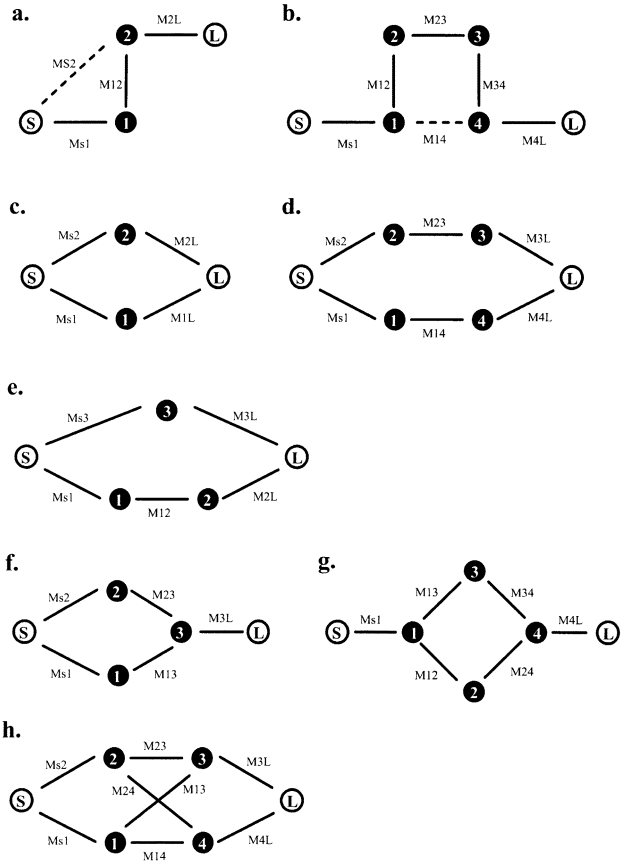

Fig. 1. Coupling schemes providing transmission zeros at finite frequencies. (a) Conventional two-pole and (b) four-pole filter designs. Pure parallel-path solutions: equal number of parallel resonances [(c) two-pole and (d) four-pole filter types], different number of resonance circuits [(e) three-pole]. Few further structures providing new filter realizations [(f) three-pole and (g), (h) four-pole filter types].

The ubiquitous direct coupling terms in microwave filters in general and multimode ones in particular arguably makes the design of these filters unnecessarily complicated at times. The first of several points addressed in this paper is the investigation of new coupling schemes for elliptic and pseudoelliptic filters in which some selected direct coupling coefficients are not present. These solutions, which may involve coupling the source and load to more than one resonator, contain more than one main path (N-path filters) for the signal between the source and load. These paths may originate at the source and terminate at the load [cf. schemes of filter examples in Fig. 1(c)–(e)] or originate and terminate between internal resonators [cf. Fig. 1(f) and (g)]. There may also be noninteracting, as in parallel realization [6], [7], or interacting through additional bypass or cross-couplings. Some of these solutions can be used to design dual-mode filters without intra-cavity couplings.

The second point addressed in this paper relates to the search for coupling schemes that allow modular design of higher order microwave filters. It will be shown that the coupling topologies introduced in this paper allow the filter designer to focus on separate sections of the structure at a time. The responses of the individual paths (sections) yield the response of the complete filter by proper superposition. Consequently, these new solutions may facilitate the realization of higher order filters by breaking them down into separate parallel sections that are designed and tuned separately and then interconnected at the interface ports.

The third point is the investigation of coupling schemes that exhibit transformation properties, whereby some characteristics of the response of the filter, such as its transmission zeros, are controlled only by parameters that can be easily adjusted. For example, we will show that some of these coupling schemes lead to pseudoelliptic filters whose transmission zeros can be shifted from one side of the passband to the other by simply changing the resonant frequencies of the resonators while leaving all the coupling coefficients unchanged.

II. Synthesis Problem

The model used for the set of coupled resonators is based on the structure proposed by Atia and Williams with proper extension to include source/load–multiresonator couplings [4]. The synthesis problem consists of determining the coupling coefficients, which are assumed frequency independent, and the frequency shifts of the resonators such that the response of the structure is identical to a prescribe elliptic or pseudoelliptic response. To this end, we use the technique presented in [8]. In this technique, the entries of the coupling matrix are used as independent variables in a gradient-based optimization technique where a sufficient cost function is used. The generality of this technique allows the investigation of new topologies for resonator filters. Details and some examples can be found in [8].

The first step in the synthesis is to select a coupling scheme (topology matrix) that is known to generate the required number of finite transmission zeros. This number can be determined using the algorithm in [9]. The choice of the topology is ultimately dictated by the limitations of the technology used for the implementation. More specifically, we are interested in synthesizing coupled resonator filters where some of the direct couplings are zero. These topologies can be used, for example, to eliminate intra-cavity couplings in dual-mode cavity filters.

Obviously, if the only concern were the elimination of some specific direct couplings, the problem would be a relatively simple exercise. What needs to be achieved is the elimination of selected direct couplings without creating new cross or bypass couplings that may not be realizable due to the constraints of a given technology. One may still argue that even this goal could be achieved in principle using a series of similarity transformations (rotations). However, there is no known approach to determine such a series beforehand in *general*. Even when a specific sequence of transformations is known, it applies only to specific coupling schemes, which is the case of some, if not all, of the coupling schemes introduced in this paper. Within such an approach, the practicing engineering is required to keep track of which sequence applies to which configuration or rely on the expertise of a handful of filter specialists. Another important point is the fact that the analytical approach using rotations can give only exact solutions. However, approximate and arguably valid solutions may be found in cases where exact solutions do not exist, as will be shown later. Consequently, we apply the technique described in [8] where the desired topology is strictly enforced, in particular, the vanishing of specific main couplings.

III. Zero-Shifting Property

An interesting property of some of the coupling schemes introduced here is the ability to shift transmission zeros from one side of the passband to the other by simply adjusting the resonance frequencies of the resonators without changing the coupling coefficients and without affecting the minimum in-band return loss of the filter. This property can be used to design filters with arbitrarily prescribed transmission zeros by cascading elemental sections that exhibit this zero-shifting property. A "doublet" [cf. Fig. 1(c)], which contains two resonators and generates one transmission zero is an example of such an elemental section. Starting from an elemental section with one transmission zero on a given side of the passband, elemental sections with transmission zeros on the other side of the passband can be designed by adjusting the resonance frequencies of the resonators to move the transmission zero and then fine optimize to finalize the design. Such a modular approach to filter design offers many advantages. First, the sensitivity of the designed filters is reduced since each elemental section controls only one transmission zero. Second, filters can be designed by starting from a single pre-designed elemental section that acts as a seed. Nearly identical filter structures can be used for generating transmission zeros at either side of the passband without any change of the coupling structure.

The zero-shifting property of some of the coupling schemes can be demonstrated rigorously using a model of the coupled resonator filter. The proof is presented for the case of the two-resonator filter shown in Fig. 1(c).

Let us denote by M_{ij} an entry of the coupling matrix that is assumed frequency independent. The loop currents, which are grouped in a vector $[I]$, are given by a matrix equation of the form [8]

$$[-jR + \Omega W + M][I] = [A][I] = -j[e], \qquad j^2 = -1. \quad (1)$$

Here, $[R]$ is a $(n+2) \times (n+2)$ matrix whose only nonzero entries are $R_{11} = R_{n+2,\,n+2} = 1$, $[W]$ is similar to the $(n+2)\times(n+2)$ identity matrix, except that $W_{11} = W_{n+2,\,n+2} = 0$, and $[M]$ is the $(n+2)\times(n+2)$ symmetric coupling matrix. The excitation vector is $[e]^t = [1, 0, 0, \ldots, 0]$. The low-pass prototype normalized frequency is denoted by Ω. Note that the coupling matrix $[M]$ may have nonzero diagonal elements, which account for differences in the resonant frequencies of the different resonators. The domain of validity of this model is explained well in [4]. The transmission coefficient S_{21} and reflection coefficient S_{11} of the model are given by (load and source resistors $= 1$)

$$S_{21} = -2j\left[A^{-1}\right]_{n+2,\,1} \quad (2)$$

and

$$S_{11} = 1 + 2j\left[A^{-1}\right]_{11}. \quad (3)$$

In this particular case [see Fig. 1(c)], the inverse of the matrix $[A]$ can be calculated analytically yielding the following result:

$$S_{21} = \frac{a\Omega + b}{\det} \tag{4}$$

$$S_{11} = \frac{\Omega^2 + c\Omega + d}{\det}. \tag{5}$$

The constants in these two equations and the determinant $\det$ are given in the Appendix. From these expressions, it is obvious that changing the signs of the diagonal elements of the coupling matrix M changes $|S_{11}(\Omega)|$ and $|S_{21}(\Omega)|$ into $|S_{11}(-\Omega)|$ and $|S_{21}(-\Omega)|$, respectively. In particular, the normalized frequency of the finite transmission zero changes sign, i.e., it moves from one side of the passband to the other. The same argument can be used to show that the coupling schemes in Fig. 1(d) and (h) also exhibit this property. Coupling schemes such as triplets, which have been used at input and output of dual-mode filters [10], [11], do not exhibit this zero-shifting property, as is easily shown following the same argument. The same holds as well for quadruplets.

IV. Synthesis Results

In the following, examples (additional to those given in [12]) are introduced in view of the outlined features above, namely, implementation of zero shifting properties, parallel path filter realizations, and new filter structures.

A. Two-Resonator Filter With One Transmission Zero

This two-pole filter example is based on the coupling scheme in Fig. 1(c). The coupling matrix

$$M = \begin{bmatrix} 0 & 0.6544 & -1.0743 & 0 \\ 0.6544 & -1.6450 & 0 & 0.6544 \\ -1.0743 & 0 & 1.4991 & 1.0743 \\ 0 & 0.6544 & 1.0743 & 0 \end{bmatrix} \tag{6}$$

exhibits identical values as given in [12, eq. (2)], but with different signs of the diagonal elements. The resulting response (Fig. 2) provides a transmission zero above the filter passband at a mirrored location compared with the respective response in [12]. Thus, this design provides a first proof of the above-mentioned zero shifting property.

B. Three-Resonator Filter With Two Transmission Zeros

The second example is a three-resonator filter with two transmission zeros in the upper stopband. The transmission zeros are located at 12.1 and 12.4 GHz. The in-band return loss is 21 dB and the bandwidth is 120 MHz centered at 11.99 GHz.

The coupling and routing scheme used for this design is given in Fig. 1(e). Two separate paths between the source and load comprise two resonators and one resonator, respectively. The coupling matrix that corresponds to these specifications is given by

$$M = \begin{bmatrix} 0.0000 & 1.0651 & 0.0000 & 0.3858 & 0.0000 \\ 1.0651 & 0.4835 & 1.1200 & 0.0000 & 0.0000 \\ 0.0000 & 1.1200 & 0.4835 & 0.0000 & 1.0651 \\ 0.3858 & 0.0000 & 0.0000 & -1.3470 & 0.3858 \\ 0.0000 & 0.0000 & 1.0651 & 0.3858 & 0.0000 \end{bmatrix}. \tag{7}$$

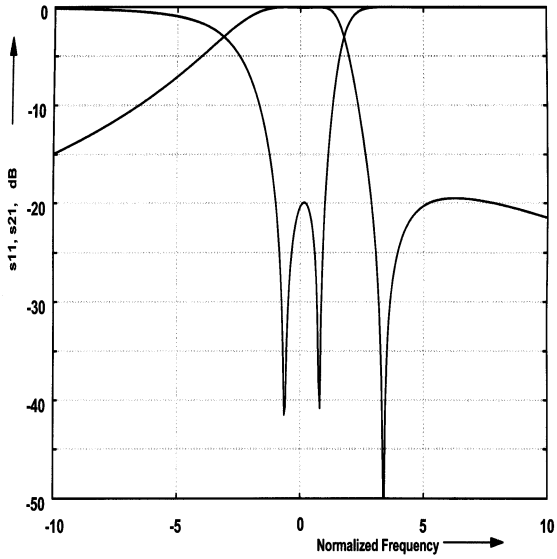

Fig. 2. Two-pole filter response with transmission zero above the passband by the change of resonance detuning.

The response of this coupling matrix, along with that obtained from the filtering function, is shown in Fig. 3. The presence of the two transmission zeros is evident.

It is interesting to examine how the transmission zeros are brought about in this case. To this end, the responses of the two separate paths in the coupling scheme are generated and plotted simultaneously in Fig. 3. It can be seen that the transmission coefficients are equal in magnitude at the positions of the transmission zeros and that their relative phase there is 180°. There are other points in the passband and in the lower stopband where the two transmission coefficients are equal in magnitude, but the relative phase condition for the generation of a transmission zero is not satisfied at these frequencies. It should be noted that there is a restriction on how close to the passband the first transmission zero is due to the large value of M_{44} in (7).

Although this structure does not exhibit the zero-shifting property of the previous case, the two transmission zeros can be shifted to the other side of the passband by changing the sign of one coupling coefficient and detuning the resonators the opposite way, i.e., changing the signs of the diagonal elements of the coupling matrix. The resulting response is indicated by the dashed line in Fig. 3(a).

A more detailed examination of the response of these two filters shows that the solution is actually not exactly equiripple although the maximum deviation between the two in-band return loss minima is only 0.2 dB. This example shows that even when an exact solution is not found, an approximate one may be perfectly valid.

C. Four-Resonator Filter With Two Transmission Zeros

An example with two two-pole filter sections in parallel according to the scheme in Fig. 1(d) is presented in [12]. It provides an elliptic function response without any detuning of the resonances as the respective coupling matrix [12, eq. (3)] shows. It is, however, worth pointing out that the fourth-order coupling structure in Fig. 1(d) implements only symmetric responses with two transmission zeros. Other four-pole designs with additional

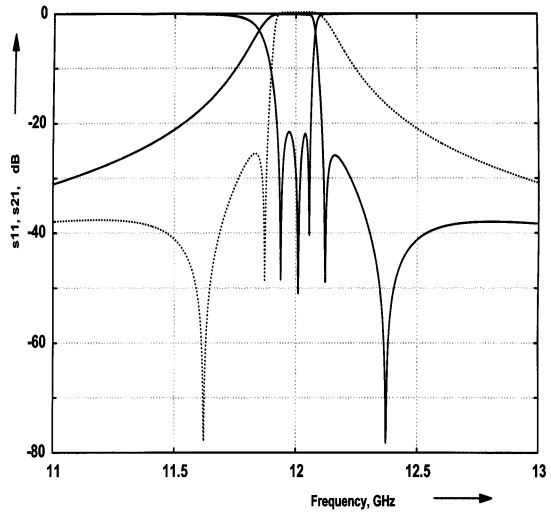

(a)

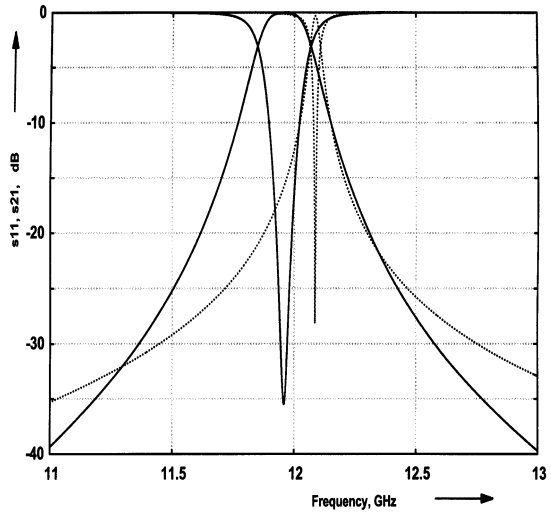

(b)

Fig. 3. Three-pole filter design according to schematic Fig. 1(e) and coupling matrix (7). (a) Response of one- and two-pole sections in parallel (dashed line shows response with changed signs in the coupling matrix—diagonal elements and one coupling sign). (b) Single responses of separate one- (dashed lines) and two-pole (solid lines) sections.

interacting couplings between the paths [according to coupling scheme Fig. 1(h)] are also introduced in [12], satisfying the identical elliptic function characteristic. These structures can also be used for arbitrary location of two transmission zeros as well. Note also that there are multiple solutions for the structures in Fig. 1(h) and Fig. 1(f). Some of these solutions are better suited for applications where certain restrictions on the internal coupling coefficients exist. Such restrictions can be easily handled within the synthesis technique used in this study [8]. For further details on these four-pole filter designs, the reader is referred to [12].

D. More Examples

For higher order filters, the pure parallel structures [see Fig. 1(c)–(e)] can be extended with additional resonance circuits in both or either one of the paths or by introducing additional paths. Another extension of design possibilities is obtained by introducing these basic structures [cf. Fig. 1(c)–(e)] as subsections in the main path of an overall filter. Thus, the parallel paths will no longer be interconnected between source and load. Fig. 1(f) and (g) shows two examples out of the variety of new possibilities. Both structures will provide one transmission zero at either side of the passband. Note that the noninteracting paths do not originate at the source and terminate at the load, as in the previous examples. The description of two quite different implementations below—using those structures—will provide an impression of the extended design possibilities and flexibility of the new approach.

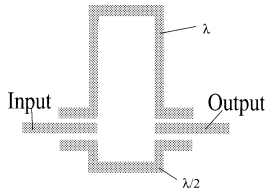

Fig. 4. Principle layout of two-pole stripline filter according to scheme Fig. 1(c).

An important point in extending the structures presented here to higher order filters relates to the sensitivity of these solutions and their limitations as to what type of transfer functions can a given coupling scheme implement exactly. These issues are not addressed in this paper, but will be the subject of a future paper.

V. Implementation

This new coupling method is not restricted to a special kind of filter realization. Therefore, different implementations are discussed for some design examples based on the coupling schemes above (cf. Fig. 1) to highlight new possibilities.

A. Two-Pole Microstrip Filter

The first example is a second-order filter with one transmission zero designed in microstrip technology. The width of the microstrip lines is 0.508 mm, the thickness of the substrate is 0.508 mm, and the dielectric constant is 10. These values are approximately those of a 50-Ω line.

The main difficulty in realizing such a filter in microstrip is the implementation of the negative coupling coefficient as needed for a design according to coupling matrix equation (6). A simple solution is the utilization of transformation properties of higher order mode resonators, similar to that introduced for waveguide resonator filters in [13]. We, therefore, use one resonator of the $\lambda/2$ type and one of the λ type, resulting in a negative coupling sign in one path. Fig. 4 shows the principle layout of such a filter. This particular layout was chosen since it allows easy control of the resonant frequencies of the two resonators by simply adjusting the lengths of the vertical branches without affecting the coupling coefficients.

The response of such a filter is shown in Fig. 5. These results were obtained from the commercial software package IE3D from Zeland Software Inc., Fremont, CA. The presence of the two reflection zeros, as well as the transmission zero, is obvious.

To confirm the zero-shifting property of this structure, the vertical lengths that control the resonant frequencies of the two

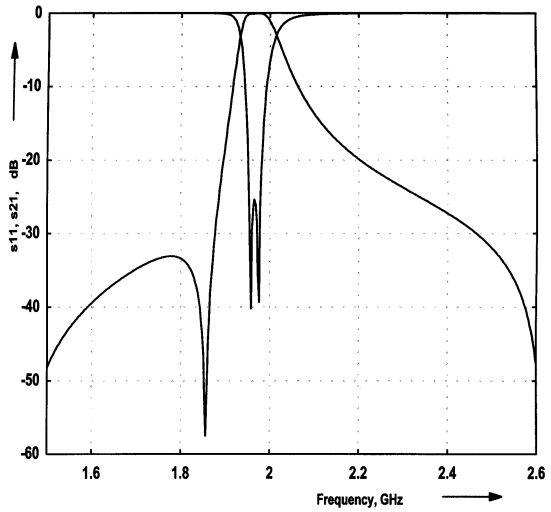

Fig. 5. Response of microstrip filter with one transmission zero in the lower stopband.

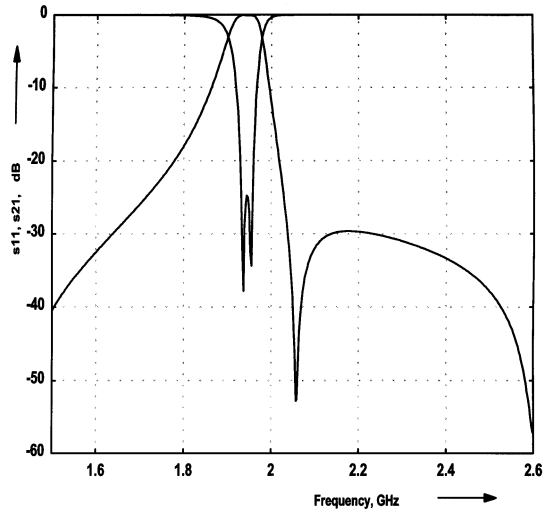

Fig. 6. Response of microstrip filter with one transmission zero in the upper stopband.

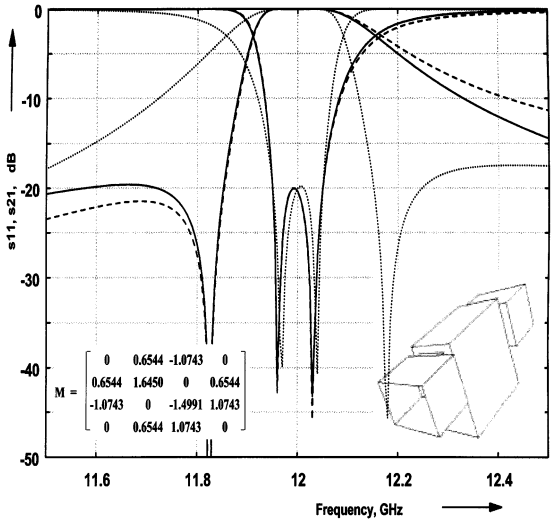

Fig. 7. Two-pole $\mathrm{TE}_{101}/\mathrm{TM}_{110}$ dual-mode filter, coupling matrix, geometric structure, (dashed lines) synthesized, and (solid lines) analyzed response. (Dotted lines: analyzed response with only changed cavity length and width dimensions.)

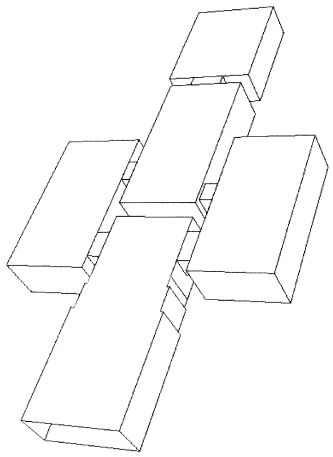

Fig. 8. Three-pole TE_{103} filter geometry according to the scheme of Fig. 1(f).

resonators were adjusted to move the transmission zero to the other side of the passband. All the remaining dimensions were left unchanged. Fig. 6 shows the response of the resulting filter. It is obvious not only that the transmission zero has moved to the other side of the passband, but that the minimum in-band return loss has not been affected—thus validating the zero-shifting property of this structure.

B. Two-Pole $\mathrm{TE}_{101}/\mathrm{TM}_{011}$ *Dual-Mode Cavity Filter*

This design is based on the same coupling structure as the microstrip type, however, it is realized by a $\mathrm{TE}_{101}/\mathrm{TM}_{110}$ rectangular dual-mode cavity at 12 GHz (100-MHz equiripple bandwidth, 20-dB return loss). Both resonances are simultaneously coupled via irises with a vertical offset from the center cavity location with waveguide interface ports (cf. sketch of the geometry in Fig. 7). Consequently, different transformation properties of resonance modes between input and output account for the opposite signs in the two separate signal paths. Note that there is no intra-cavity coupling of the resonances. The design of the physical filter structure has been performed to satisfy the synthesized response (dashed lines and coupling matrix) in Fig. 7. The results of the computation with a mode-matching method yield good coincidence of synthesized and analyzed responses up to three times the filter bandwidth below and above the passband. The increasing deviation of the responses outside that frequency band can be attributed to the mode dispersion effects of the cavity.

The zero shifting property has also been verified by this structure by only changing the width and the length of the cavity. The dotted lines show the response of that filter, which corresponds to the predicted characteristic with the transmission zero above the passband.

C. Three-Pole Waveguide Cavity Filter

This filter design is based on the coupling scheme in Fig. 1(f). It has been realized at 38.42 GHz (60-MHz equiripple bandwidth, 20-dB return loss) with one transmission zero at 38.25 GHz—using TE_{103}-mode cavities. The cavity structure is depicted in Fig. 8. The input waveguide is short circuited at

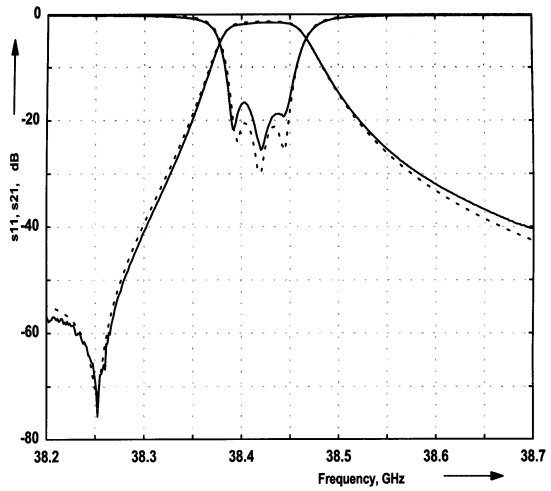

Fig. 9. Measured (solid line) and synthesized (dashed lines) responses of the three-pole TE_{103} cavity filter.

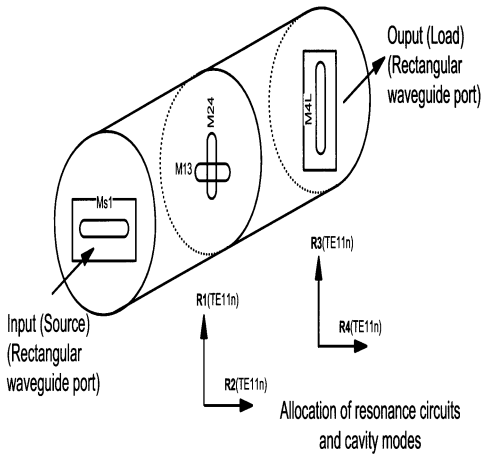

Fig. 10. Principle structure for a four-pole dual-mode filter design according to the scheme of Fig. 1(g).

one end and couples via inductive irises the first field maximum of the TE_{103} cavities 1 and 2 of the filter at its sidewalls. Inductive irises are also used to couple these cavities with the third cavity, which is aligned on axis with the interface waveguides. To account for the needed different coupling signs in this filter section, the transformation properties of TE_{103} mode are utilized, i.e., the third maximum of cavity 1 is coupled to the first one of cavity 3, while the second maximum of cavity 2 is also coupled to the first maximum of cavity 3 (cf. [13]). The wall of cavity 3 opposite to the input interface location of the filter is facing the output waveguide via an iris. This filter has been designed using a mode-matching method. Based on these results, it has been realized with tuning means for couplings and resonances, which is common for filters with such extreme narrow bandwidth ($<$0.2%). Measured and synthesized responses, depicted in Fig. 9, agree closely and also prove the design approach. The zero shifting property can also be verified by this structure, which is mainly attributed to the detuning of cavities 1 and 2.

D. Four-Pole Dual-Mode Filter

The last example concerns the description of a four-pole dual-mode in-line filter design according to the coupling structure shown in Fig. 1(g). The principle geometry and assignment of the degenerate TE_{11n} cavity modes to the filter resonance circuits is displayed in Fig. 10.

The TE_{10} waveguide modes at the rectangular waveguide interface ports are coupled via inductive irises with the TE_{11n} resonance modes (exhibiting the respective polarization) of the adjacent cavities that represent filter circuits R_1 and R_4. The main signal path of the filter is split into two parallel sections between resonance circuits R_1 and R_4. Thus, one of the two separate sections is formed by the resonance circuit R_2 with the dedicated couplings M_{12} and M_{24}, and the second one consists of resonance circuit R_3 with assigned couplings M_{13} and M_{34}. Hence, resonance circuit R_1 is simultaneously coupled to the degenerate TE_{11n} mode (with orthogonal polarization) of the same cavity (representing R_2) by a screw (not shown in Fig. 10) and the respective TE_{11n} mode (R_3) of the adjacent cavity (having the same polarization) by an iris (M_{13}). Resonator R_4 is coupled in the same manner with R_3 by a screw M_{34} and R_2 by an iris.

The second resonance circuit R_2 is represented by the orthogonal polarized degeneracy of the first physical cavity. However, the third resonance (R_3) is dedicated to that degeneracy of the second cavity having the same polarization as the first resonance circuit (R_1), in contrast to state-of-the-art dual-mode filters, where first and third resonance circuits exhibit orthogonal polarization. It should be noted that this new four-pole filter structure provides input and output waveguide ports with perpendicular alignment (due to the orthogonal polarization of first and fourth resonance circuits) in contrast to a conventional four-pole dual-mode filter design (cf. [4]).

This particular design allows the realization of one transmission zero arbitrarily located below or above the filter passband—which can also be tuned to either side of the passband by the zero shifting property. Consequently, it is substantially simpler than that given by Cameron in [14].

Please note, inter-cavity iris couplings are only performed between equal polarized TE_{11n} modes (there is no coupling between the two main coupling paths, i.e., resonance circuits 2 and 3), which allows plain iris designs—in contrast to Cameron's design, which needs special angular aligned irises between the dual-mode cavities [14].

VI. Conclusions and Outlook

Novel solutions to the synthesis problem of coupled resonator elliptic filters have been presented. A salient feature of these solutions is the fact that some of their direct (main) couplings are zero. These solutions contain two or more main paths for the signal between the source and load. It is shown that higher order filter responses can be obtained by separate parallel connected lower order filter sections between source and load ports due to proper superposition of the different responses of the individual sections. Special parallel filter sections with zero shifting properties may be implemented in higher order filter designs to facilitate the design of arbitrary filter responses. Some design examples and descriptions dedicated to different realizations—from

microstrip to dual-mode cavity filter types—give a small impression of the broad spectrum of new possibilities offered by the introduced method.

APPENDIX

Here, we give the expressions of the coefficients in the scattering parameters given in (4) and (5).

We assume that the coupling matrix is of the form

$$M = \begin{bmatrix} 0 & x_1 & x_3 & 0 \\ x_1 & x_5 & 0 & x_4 \\ x_3 & 0 & x_6 & x_2 \\ 0 & x_4 & x_2 & 0 \end{bmatrix}. \tag{A.1}$$

Using this matrix, the coefficients in (4) and (5) are given by

$$a = -x_2x_3 - x_1x_4 \tag{A.2}$$

$$b = -x_2x_3x_5 - x_1x_4x_6 \tag{A.3}$$

$$c = x_5 + x_6 + j\left(x_1^2 - x_2^2 + x_3^2 - x_4^2\right) \tag{A.4}$$

$$d = x_5x_6 - 2x_1x_2x_3x_4 + x_1^2x_2^2 + x_3^2x_4^2 + jx_5\left(x_3^2 - x_2^2\right) + jx_6\left(x_1^2 - x_4^2\right) \tag{A.5}$$

$$\det = -\Omega^2 + e\Omega + f \tag{A.6}$$

$$e = -(x_5 + x_6) + j\left(x_1^2 + x_2^2 + x_3^2 + x_4^2\right) \tag{A.7}$$

$$f = -x_5x_6 - 2x_1x_2x_3x_4 + x_1^2x_2^2 + x_3^2x_4^2 + jx_5\left(x_3^2 + x_2^2\right) + jx_6\left(x_1^2 + x_4^2\right). \tag{A.8}$$

From these equations, it is evident that changing x_5 and x_6 into $-x_5$ and $-x_6$ changes the *magnitudes* of $S_{11}(\Omega)$ and $S_{21}(\Omega)$, as given by (4) and (5), into the *magnitudes* of $S_{11}(-\Omega)$ and $S_{21}(-\Omega)$, respectively.

ACKNOWLEDGMENT

The authors thank the anonymous reviewer of this paper's manuscript for very constructive comments, as well as for pointing out that, in [12], coupling matrix (4), M_{22} should be negative.

REFERENCES

[1] R. J. Cameron, "General coupling matrix synthesis methods for Chebyshev filtering functions," *IEEE Trans. Microwave Theory Tech.*, vol. 47, pp. 433–442, Apr. 1999.

[2] ——, "General prototype network synthesis methods for microwave filters," *ESA J.*, vol. 6, pp. 193–206, 1982.

[3] R. J. Cameron and J. D. Rhodes, "Asymmetric realizations of dual-mode bandpass filters," *IEEE Trans. Microwave Theory Tech.*, vol. MTT-29, pp. 51–58, Jan. 1981.

[4] A. Atia and A. Williams, "New type of waveguide bandpass filters for satellite transponders," *COMSAT Tech. Rev.*, vol. 1, no. 1, pp. 21–43, 1971.

[5] G. Pfitzenmaier, "Synthesis and realization of narrow-band canonical microwave bandpass filters exhibiting linear phase and transmission zeros," *IEEE Trans. Microwave Theory Tech.*, vol. MTT-30, pp. 1300–1311, Sept. 1982.

[6] A. Matsumoto, *Recent Advances in Microwave Filters and Circuits*. New York: Academic, 1970.

[7] V. Osipenkov and S. G. Vesnin, "Microwave filters of parallel cascade structure," *IEEE Trans. Microwave Theory Tech.*, vol. 42, pp. 1360–1367, July 1994.

[8] S. Amari, U. Rosenberg, and J. Bornemann, "Adaptive synthesis and design of resonator filters with source/load-multi-resonator coupling," *IEEE Trans. Microwave Theory Tech.*, vol. 50, pp. 1969–1978, Aug. 2002.

[9] S. Amari and J. Bornemann, "Maximum number of finite transmission zeros of coupled resonator filters with source/load-multi-resonator coupling and a given topology," in *Proc. Asia–Pacific Microwave Conf.*, Sydney, Australia, 2000, [Online]. Available: http://www.ece.uvic.ca/~bornema/publicat.html, pp. 1175–1177.

[10] L. Accatino, G. Bertin, M. Mongiardo, and G. Resnati, "A new dielectric-loaded dual-mode cavity for mobile communications filters," in *31st Eur. Microwave Conf.*, vol. 1, Sept. 2001, pp. 37–40.

[11] I. C. Hunter, J. D. Rhodes, and V. Dassonville, "Dual-mode filters with conductor-loaded dielectric resonators," *IEEE Trans. Microwave Theory Tech.*, vol. 47, pp. 2304–2311, Dec. 1999.

[12] U. Rosenberg and S. Amari, "Novel coupling schemes for microwave resonator filters," in *Proc. IEEE MTT-S Int. Microwave Symp.*, Seattle, WA, May 2002.

[13] U. Rosenberg, "New 'planar' waveguide cavity elliptic function filters," in *Proc. 25th Eur. Microwave Conf.*, vol. 42, no. 7, Bologna, Italy, Sept. 1995, pp. 524–527.

[14] R. J. Cameron, "Dual-mode realizations for asymmetric filter characteristics," *ESA J.*, vol. 6, pp. 339–356, 1982.

Uwe Rosenberg (M'90–SM'93) received the Dipl. Ing. degree (first-class honors) in electrical engineering (telecommunication technique) from the Fachhochschule der Deutschen Bundespost, Dieburg, Germany, in 1982.

From 1982 to 1983, he was with Hydro Therm, Dieburg, Germany, where he was involved with the design and development of automatic safety and heating control circuits. From 1983 to 1985, he was with the Technische Hochschule Darmstadt, Darmstadt, Germany, where he was involved with the design and development of experimental installations and software components for microcomputer control systems. In 1985, he joined the Space Division, ANT Nachrichtentechnik GmbH (now Tesat-Spacecom GmbH & Company KG), Backnang, Germany, where he was engaged in research and development on microwave filters, multiplexers, and passive subsystems for communications satellites. Since 1989, he has been Head of the Research and Development Laboratory for Passive Microwave Components and Subsystems, Marconi Communications GmbH (formerly Bosch Telecom GmbH, Public Networks Division), Backnang, Germany, where he has been responsible for research and development of integrated waveguide transceiver circuitries, channel branching networks (multiplexers), antenna feed and waveguide (feeder) systems for trunk and access radio applications, mobile base-stations, large Earth stations, and communications satellites. He coauthored *Waveguide Components for Antenna Feed Systems: Theory and CAD* (Norwood, MA: Artech House, 1993). He has also authored or coauthored over 50 technical papers. He holds 36 microwave design patents

Mr. Rosenberg is a member of Verband der Elektrotechnik Elektronik Informationstechnik (VDE), Informationstechnische Gesellschaft (ITG), and Verein Deutscher Ingenieure (VDI). He is a senior member of the IEEE Microwave Theory and Techniques Society (IEEE MTT-S) and the IEEE Antenna and Propagation Society (IEEE AP-S).

Smain Amari (M'98) received the DES degree in physics and electronics from Constantine University, Constantine, Algeria, in 1985, and the Masters degree in electrical engineering and Ph.D. degree in physics from Washington University, St. Louis, MO, in 1989 and 1994, respectively.

From 1994 to 2000, he was with the Department of Electrical and Computer Engineering, University of Victoria, Victoria, BC, Canada. From 1997 to 1999, he was a Visiting Scientist with the Swiss Federal Institute of Technology, Zurich, Switzerland, and a Visiting Professor in Summer 2001. Since November 2000, he has been with the Department of Electrical and Computer Engineering, Royal Military College of Canada, Kingston, ON, Canada, where he is currently an Associate Professor. He is interested in numerical analysis, numerical techniques in electromagnetics, applied physics, applied mathematics, and quantum many-particle systems.